EpiBOX: A Novel Approach to Long-Term Data Acquisition with Automatic Seizure Detection in Epilepsy

Ana Sofia Cacais do Carmo
ana.sofia.carmo@tecnico.ulisboa.pt

Instituto Superior Técnico, Lisboa, Portugal

January 2021

Abstract

Epilepsy is a neurological disease that affects about 50 million people worldwide, and around 50 thousand in Portugal alone. It is a disorder of the central nervous system, characterized by recurrent seizures that can have a massive impact in the physical and mental health of the people who suffer from it, as well as their loved ones.

Research is an invaluable tool in the improvement of conditions for clinicians and patients to deal with epilepsy. However data is key, and it is not always available, at least not in the desired conditions. Accordingly, this work proposes a practical alternative for the acquisition of biosignals using wearable devices, with the ultimate goal of providing a fully automated seizure detection system, for scalable long-term dataset creation.

EpiBOX was conceived as a practical and standalone multimodal acquisition system with capacity for acquiring, displaying and storing up to 12 different channels, simultaneously, with a simple interaction framework. Additionally, a seizure-specific SVM classifier was designed for eight different types of seizure, using a limited-channel configuration (*Fp1-Fp2*). The dataset used was TUH EEG Seizure Corpus, for which phenomenal results were achieved for tonic-clonic and myoclonic seizures, with sensitivities of 98.9% and 98.2%, as well as precisions of 100% and 99.8%, respectively.

This dissertation provides important ground work for larger collaborative projects in the field of epilepsy and others, serving both as a complementary tool for research, as well as first steps for some technological solutions.

Keywords: epilepsy, seizure detection, EEG, biosignal acquisition, BITalino, Raspberry Pi

1. Introduction

According to the World Health Organization (WHO), 50 million people worldwide, and 50 thousand people in Portugal, suffer from epilepsy, a noncommunicable neurological disease that can affect people of all ages.

This condition can have tremendous effects on the lives of the people who suffer from it and the people close to them, either due to the health impacts it carries, such as the physical impairments that can result from a seizure and the increased risk of other chronic health conditions; or due to the socio-economic burden it often brings.

Research in biomedical signals and systems has an invaluable role in the evolution of how patients and clinicians deal with epilepsy (as in any other medical condition), as it can provide novel tools to diagnose, monitor and manage the condition. An essential agent in research is data and, in some cases, it is not easily available. In epilepsy, there are several available open-access online datasets (such as CHB-MIT [15] and TUSZ [13]), however, each dataset has its own singularities, either regarding seizure type, demographics of the subjects, annotations, etc.

Moreover, the COVID-19 pandemic mitigation measures introduced additional difficulties for the management of the disease. In particular, there has been a significant decrease between in the patient-clinician encounters and inpatient visits for long-term monitoring. This created a pressing need for new ways of facilitating wearable and practical patient monitoring, especially based on remote and automated minimally-assisted methods.

Therefore, the purpose of this work is to create an autonomous system for continuous or near-continuous data acquisition using wearable devices (*EpiBOX*) and a seizure detection algorithm. This is a necessary stepping stone to

achieve the ultimate goal of providing a fully automated seizure detection system, which will enable scalable long-term dataset creation containing in-hospital and at-home recordings, both longitudinal and cross-sectional [3]. Moreover, *EpiBOX* is not limited to seizure detection and Electroencephalography (EEG) acquisition. It is designed as a versatile acquisition system, that can record multimodal biosignal data, and can be integrated with whichever Machine Learning (ML) algorithm.

2. Background

According to the WHO, epilepsy is characterized by recurrent seizures, which are sudden and uncontrolled disturbances in the electrical activity of the brain. However, a single seizure does not imply epilepsy, but rather it is diagnosed only in the event of at least two unprovoked seizures.

In epileptic seizures in particular, there are three distinctly relevant features: the seizure focus (i.e. the region of the brain where the sudden excessive electrical discharge started), how far it spreads across the brain and the symptoms it causes. In focal (or partial) seizures, the focus is confined to a specific region of the brain (and may spread from there), whereas in generalized seizures the excessive electrical discharge starts virtually simultaneously across the brain. Table 1 describes the different seizure types within these two categories, and based on the three key features.

Table 1: Types of seizures within generalized and focal seizures, along with a description and common manifestations. Source: Ochal et al. (*The Temple University Hospital EEG Corpus: Annotation Guidelines*, 2020)

Seizure Type	Description
Tonic	Associated with stiffening of the muscles and impaired consciousness.
Clonic	Sustained, rhythmic jerking and potential loss of consciousness, followed by confusion.
Tonic-clonic	Involves loss of consciousness and violent muscle contractions.
Atonic	Involves the loss of tone of muscles in the body.
Myoclonic	Results in brief involuntary twitching or myoclonus.
Absence	Involves lapse in attention, may result in impaired memory.
Simple partial	Onset in one location of the brain (with the possibility of spreading). Usually brief, characterized by full awareness but may cause sensory responses.
Complex partial	Same as simple focal, but characterized by impaired awareness.

3. State-of-the-Art

Automated Electroencephalography (EEG) analysis for the detection of epileptic seizures is extensively studied in literature, encompassing several feature extraction techniques and machine learning methods, many of which show satisfactory performances. However, high-density EEG acquisition is only reasonable in clinical settings. There is some literature researching the channels/montages that might be more significant for the task of seizure detection, with the purpose of limiting their use for wearable version of the acquisition.

This type of study can be performed using, for example, filter methods in order to find the most relevant/informative channels and filtering out the remaining [5] or wrapper-based methods (such as backward-elimination) to identify the subset of channels that provide the best seizure detection performance [10].

Alternatively, a subset of channels can be predetermined based on domain knowledge and its predictive power can be estimated directly from its performance on seizure detection. Both Lin et al. [8] and Sopic et al. [16] conducted similar studies, but with different numbers of channels. Lin et al. reported an average detection rate of 92.68% and False Positive Rate (FPR) of 0.527/h for channel *Fp2-F8*; and Sopic et al. achieved similar results, with average sensitivity of 93.80% and specificity of 93.37%, using channels *F8-T4* and *F7-T3*.

Peterson et al. [11] suggested an interesting approach for the detection of absence seizures, in particular, investigating the detection performance of single channels (in absence seizures), from a set of 18 channels. Their findings indicate that frontal channels are overall better at discriminating this type of seizures. The authors reported that the best overall channel was *F7-FP1* (with a sensitivity of 99.1% and a FPR of 0.5/h), followed by *F7-F3* (with the same sensitivity but with a FPR of 1.0/h). *Fp1-Fp2* (which is particularly relevant for this work) also achieved a reasonable performance (with a sensitivity of 93.7% and FPR of 1.4/h).

4. *EpiBOX* - Biosignal Acquisition Setup

The designed setup for long-term biosignal acquisition is composed of three main elements, which interact through different routes/mechanisms: 1) An autonomous recording unit; 2) A biosignal acquisition system; and 3) A mobile app. The setup is responsible for performing signal acquisition, storing the acquired signal and providing its visualization to the user. Figure 1 illustrates the elements involved in the setup and the communication channels between each.

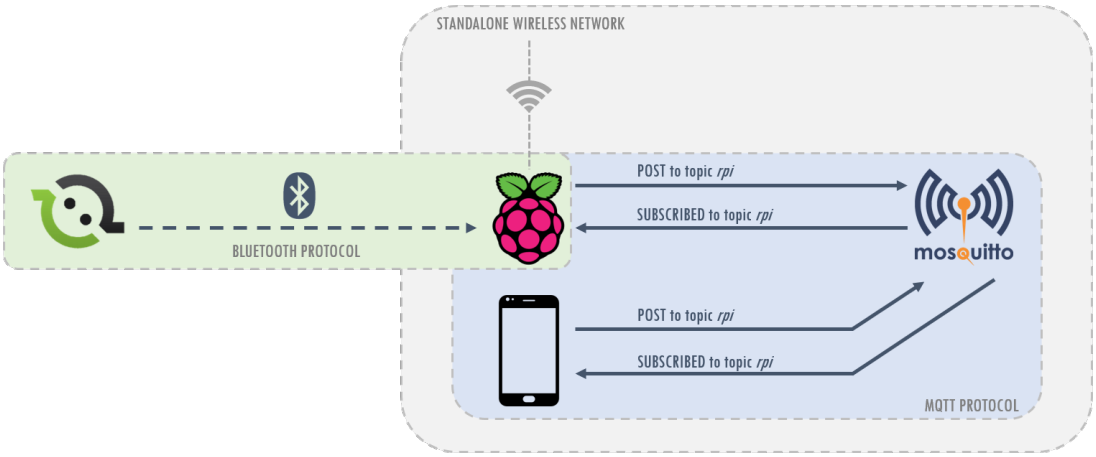

Figure 1: Architecture of the proposed system: elements involved and communication channels between each element. The area colored in green corresponds to the communication channel between the RPi and the acquisition devices (Bluetooth); the area colored in blue corresponds to the communication channel between the RPi and the mobile app (MQTT), which is purposefully contained within the grey colored area (wireless network).

4.1. Elements of *EpiBOX*

Autonomous recording unit: The autonomous recording unit is based on a Raspberry Pi (RPi), which is a tiny, single-board computer that provides a good trade-off between portability and processing power, for this particular application. It acts as the main driver of the whole system, being the sole communication agent with the biosignal acquisition system and being responsible for the launching and maintenance of the communication channel with the mobile app. The mobile app acts as a user-friendly interface with the headless RPi through a pre-defined set of messages that trigger certain actions on the RPi (e.g. which channels to acquire or when to start the acquisition). These messages are exchanged between the two elements through a MQTT protocol.

MQTT however, is built upon a wireless network, which would be naive to expect to have available in every home/hospital environment. Hence, the RPi guarantees the setup of a standalone network.

Biosignal acquisition system: For data acquisition, this work builds upon previous and ongoing work from the Pattern and Image Analysis (PIA-Lx) research group, at Instituto de Telecomunicações (IT), and uses BITalino. BITalino is a hardware and software toolkit, specifically designed to acquire body signals, which has demonstrated to be a valid equipment for research [4], superior to several of its counterparts [7]. It allows the flexibility of connecting several different sensors beyond EEG (e.g. Electrocardiography (ECG), Electrodermal Activity (EDA), and several others); as well as enabling the reconfiguration of the setup to different physical formats.

The device provides the raw signals produced by the analog-to-digital converter, which can be easily accessed - a crucial feature for the development of *EpiBOX*. Furthermore, it allows for easy interoperability with a range of platforms, including RPi, and provides an easy-to-use Python module. The connection of the RPi to each BITalino is configured whenever the acquisition process is triggered, through the methods provided in this module.

An invaluable component of this toolkit is the Bluetooth module, that acts as the communication channel between the BITalino and the RPi, allowing for real-time wireless data streaming. For the purpose of this work, considering that each BITalino allows to acquire up to 6 analog channels simultaneously and synchronously, a maximum of 2 devices were accounted for.

Communication protocol: MQTT is an extremely lightweight and reliable communication protocol. It is particularly suitable for event-driven machine-to-machine communication, making MQTT very fit for our purpose of communicating between the Raspberry Pi and the mobile phone [1].

For this work, the RPi was set as the MQTT broker, launching it on boot on the local network. Both the RPi (as a client) and the mobile phone connect to the broker, protected by password, and subscribe to the topic *"rpi"*, ensuring communication between the two, while increasing the privacy of the transaction. This architecture corresponds to the right portion of the illustration of the setup (Figure 1).

Standalone wireless network: For the communication between the devices to be settled, there needs to be a network available, which is responsible for providing the environment in which the MQTT protocol is established and can create the

[1] The fact that the communication between the Raspberry Pi and the mobile phone is entirely based on rather short strings, further enhances the suitability of MQTT protocol.

channel for the message exchange. The Raspberry Pi was configured to work as a wireless access point to run a separate, private network. Without access to the Ethernet, the RPi can not provide access to the internet, however, for this particular setup, this acts as an advantageous asset; it provides the means needed to set the MQTT channel within the network, while enhancing the overall security. For an additional layer of security, connection to this network is password protected.

4.2. Data Storage and Visualization

In every acquisition with this setup, there are two major procedures happening: the storing of the acquired data in a *.txt* file (saved with the identification of the patient and the acquisition session) and the real-time plotting of the acquired data whenever the user accesses the mobile app. They happen concurrently with the actual acquisition by the BITalino device(s).

Storing: While the BITalino device acquires data, the developed software receives it in batches of 100 samples on the Raspberry Pi, to avoid the computationally expensive process of sending one sample at a time through Bluetooth. The RPi organizes and concatenates the data from the multiple BITalino devices (if that is the case), which is then saved in the corresponding *.txt* file. This file includes a description header that contains all the information needed to interpret the data saved, such as the MAC address of each BITalino, the channels acquired from each, the signal being acquired, and other relevant settings

Visualization: The first step towards visualization is the decimation of the data, applied to each batch of 100 samples. This procedure is required to allow for proper display of the signals, further explained below. The target sampling rate is 100 Hz, which represents a significant subsampling compared to the usual 1000 Hz used for physiological signals, while at the same time preserving the most significant frequencies of each type of signal.

As in any system, both the hardware and software are not 100% reliable, and in a setup like this one, in which several components and systems are involved, the probability of error occurrence is not negligible. Hence, the setup provides the user some insight on the acquisition process, by allowing near-to real-time visualization of the signal being acquired. Every time a new set of samples is received by the mobile app, each channel is gone through and each sample point is individually drawn in the corresponding plot.

The number of points simultaneous points displayed in each plot is in fact dependent on the device hosting the mobile app, as it corresponds to the available width for the plot, i.e. the number of samples corresponds to the number of pixels (which, in turn, establishes the time interval of the signal that the user can visualize at any given instant, as described in (1)). With this implementation, we guarantee optimal adaptability for every mobile device and, most importantly, that there is not an excess amount of points being drawn without any practical effect on visualization.

$$t_{interval} = \frac{width_{(plot)}}{sampling\ rate} \tag{1}$$

5. Characterization of *EpiBOX*

Table 2: Characteristics obtained for *EpiBOX*, where the first two sections correspond to a trial acquisition of approximately 10 hours (with $\sim$5 minutes of active screen time) and the last one corresponds to inherent communication properties of *EpiBOX* (estimated for optimal conditions, without any physical barriers).

Memory usage	App: 87.97 MB Data: 46.55 MB
Energy consumption	17.93 mAh
Frame rendering	w/ visualization: 30.3 ms w/o visualization: 9.9 ms
Acquisition duration	10 h, 15 min and 35.7 s
Total samples	Expected: 36 935 687 Actual: 36 827 800
# Lost samples in batch	0
# Files	Expected: 11 Actual: 12
File durations	(51$\pm$16) min and (9$\pm$19) s
File sizes	(110 $\pm$ 41) MB
Bluetooth range	$\sim$10 m
WiFi speed	72 Mbps
WiFi strength	-30 dBm

Overall, *EpiBOX* exhibits satisfactory properties, particularly regarding the acquired data and the communication channels (see Table 2), adequate for application in a hospital/home environment. Moreover, one of the advantages of *EpiBOX*, which is not explicit in the Table, is the security of the data transfer, considering it is executed through a private network, not connected to the internet.

5.1. EEG Acquisition Wearable

Part of the purpose of this work is to develop a seizure detection algorithm that can be integrated with *EpiBOX* for a continuous monitoring, and simultaneous event detection. EEG is a gold-standard in the analysis of epilepsy, particularly in the detection and prediction of seizures. As such, we required a wearable device for the acquisition of this biosignal, that could be directly implemented with *EpiBOX*.

EmotAI's headband was specifically designed for Esports analytics (namely cognitive, emotional and behavioral), however, it has potential for use in other areas, such as epilepsy. It provides the recording of 2-channel EEG, through 2 pairs of dry electrodes positioned to acquire the channels corresponding to *Fp1* and *Fp2*. It also has an additional electrode, connected to the left ear, that acts as reference and allows to decrease noise and artifacts (the patterns that are common between the reference and the main electrodes), as well as a Photoplethysmography (PPG) sensor. The limited-channel configuration that EmotAI provides is particularly suitable for the goals of this work as it enables a relatively discreet approach for continuous monitoring of EEG. Moreover, EmotAI's headband is based on BITalino, which guarantees the necessary scientific rigor of measurements, as well as a seamless integration with *EpiBOX* without any adaptation needed.

6. Seizure Detection Algorithm

Due to COVID-19 restrictions, it was not possible to collect real-world data in the context of this work, hence, an external dataset was used (and adapted) to act as a proof of concept of the acquisition of EEG data using EmotAI's headband, and simultaneous automatic seizure detection.

6.1. Data and Preprocessing

Dataset: The TUH EEG Seizure Corpus [13] was used, one of the largest publicly available archive of clinical scalp-EEG, created by Temple University Hospital. The use of this database was only possible due to the participation in the Neureka 2020 Epilepsy Challenge. The database consists of approximately 504 hours of scalp-EEG recordings ($\sim 7\%$ corresponding to seizures), from 692 patients and containing more than 3000 seizures, all manually annotated. The dataset uses 2 different references for the recordings: Average Reference (AR) montage uses the average of a certain number of electrodes as the reference, whereas Linked-Eears Reference (LE) uses a lead adapter to link both ears, using this as reference [6]. Two montages are defined, based on the reference electrode used: *0103* (AR) and *02* (LE).

The annotations (provided as a *.txt* file for each acquisition file) in TUSZ contain 12 different labels: Focal Non-Specific Seizures (FNSZ), Generalized Seizures (GNSZ), Simple Partial Seizures (SPSZ), Complex Partial Seizures (CPSZ), Absence Seizures (ABSZ), Tonic Seizures (TNSZ), Clonic Seizures (CNSZ), Tonic-Clonic Seizures (TCSZ), Atonic Seizures (ATSZ), Myoclonic Seizures(MYSZ), and Non-Epileptic Seizures (NESZ). Non-seizure events are annotated as Background (BCKG).

Re-referencing: As mentioned, the algorithm will be designed as a proof of concept of seizure detection using EmotAI's headband, therefore only two channels will be extracted from the acquisition files, stored in European Data Format (EDF): *Fp1-REF* and *Fp2-REF*. For all acquisition files, in both datasets (*0103* and *02*), the channels *Fp1-REF* and *Fp2-REF* were extracted and re-referenced to *Fp1-Fp2*, as in (2), timestamp-wise, resulting in a single channel. In theory, this re-referencing to a common montage would be enough to cancel the effects of the different reference points; however, it is important to note that, in practice, this might not be the case: the reference point can have a major impact on the nature of the waveforms, due to the nonlinearity of the brain and scalp conduction paths [9]. As such, the potential effect of the initial reference will be analyzed during this work.

$$(Fp1 - REF) - (Fp2 - REF) = Fp1 - Fp2 \quad (2)$$

Denoising: It is known that filtering can cause significant distortion of the signal, hence why many researchers choose to skip this preprocessing step [18]. However, low-frequency noise is usually the predominant source of noise in electrophysiological data [18] and can have a major impact in the extraction of features (particularly spectral ones). All recordings were filtered using an 8-order high-pass filter, with cutoff frequency of 0.8 Hz and an 16-order lowpass filter, with cutoff frequency of 48 Hz. Note that the choice of 0.8 Hz for the cut-off frequency is slightly above the recommended in [18]. However, it was a conscious decision, as it allows to not only remove the unwanted, low-frequency, noise components, but also to approximate the range of frequencies of the TUSZ recordings to the one EmotAI's headband is able to acquire (considering BITalino's EEG bandwidth).

Signal segmentation and feature extraction: Regarding the length of the epochs, there is some degree of variety across literature, where it is suggested a trade-off between avoiding non-stationarity (too long epochs) and not overlooking important information (too short epochs that can not capture lower frequency patterns). However most agree on a reasonably short epoch. For example, neurologists typically analyze EEGs in windows of 10 seconds and identify events with a temporal resolution of $\sim$1 second [12]. Hence, each recording was split into into non-overlapping epochs, with duration of 1 second. The complete set of extracted features for each epoch, composed of nonlinear features (Higuchi Fractal Dimension, Sample Entropy and Hurst Exponent) and DWT-based features (enumerated in Table 3) corresponds to a single feature vector concatenated to form a single array of dimension $1 \times 28\ features$.

Table 3: List of features extracted for each epoch in the scope of this work. RE: Relative Energies, Mean: Mean of DWT coefficients, Std: Standard deviation of coefficients, Kurt: Kurtosis of coefficients, Skew: Skewness of coefficients. cA*n*: approximate coefficients from level *n*, cD*n*: detail coefficients from level *n*.

DWT-based				
RE	**Mean**	**Std**	**Kurt**	**Skew**
re_{cD2}	$mean_{cA5}$	std_{cA5}	$kurt_{cA5}$	$skew_{cA5}$
⋮	$mean_{cD5}$	std_{cD5}	$kurt_{cD5}$	$skew_{cD5}$
re_{cD5}	⋮	⋮	⋮	⋮
re_{cA5}	$mean_{cD2}$	std_{cD2}	$kurt_{cD2}$	$skew_{cD2}$

6.2. Sample Preprocessing and Feature Selection

Train-test split: Targeting the implementation of an online algorithm (that may have temporal constraints in its final classification state), it is preferable to test the performance in an online format as well. However, in order to do so, the test samples must be consecutive and have a temporal dependency. Hence, an alternative splitting mechanism was applied, based on an exhaustive search technique, which aims at finding the best combination of recording sessions that yields a balanced test subset, with approximately 20% of seizure samples.

Feature selection: For the purpose of this work, two main criteria were used for the filter selection method: linear separability and differential spread. Statistical methods that assume specific conditions (e.g. normal distribution) are not suitable for this particular application, given that it can not be guaranteed for all the variables under study. Hence, an alternative method was used - *overlap coefficients* - that measures the overlap of the histograms of both classes (background and seizure).

Figure 2 illustrates the results obtained for montage *02*. CPSZ is the seizure type which shows the largest overlap between the two distributions across all features, which is not very promising in terms of their usability for the upcoming task. ABSZ, TCSZ (except between std_{cD4} and $skew_{cA5}$) and MYSZ on the other hand, show much more promising results, as we can see from the consistently lower $c_{overlap}$ values. The set of ultimately selected features for montage *02* are identified with a white asterisk.

Outlier removal and feature scaling: Outliers can be particularly harmful when scaling with a bounded range is performed prior to training, hence why outlier removal is a crucial step in the context of this work. This was performed through the Interquartile Range method (illustrated in (3)).

$$IQR = Q3 - Q1$$
$$outliers : x < Q1 - 3 \times IQR \;||\; x > Q3 + 3 \times IQR \quad (3)$$

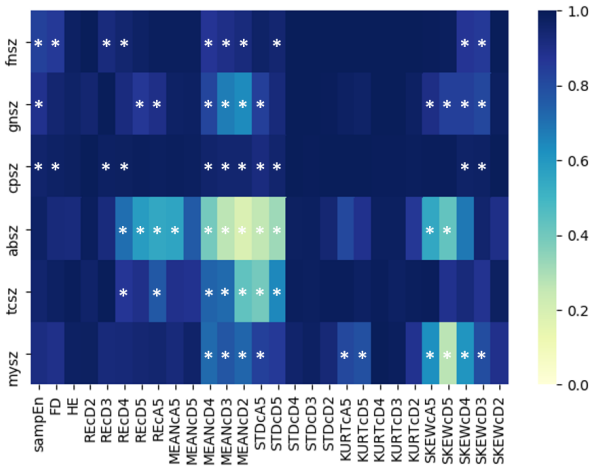

Figure 2: Heatmap with the coefficients of overlap between the distributions of background and the respective seizure. Rows correspond to the different seizure types and columns correspond to set of extracted features. Extracted from dataset *02*.

Each feature was also standardized (i.e. 0 mean and unit variance) prior to model training, using *sklearn*'s `StandardScaler()`.

6.3. Classifier

Offline training: For each montage and each seizure type, a Support Vector Machine (SVM) classifier, with Radial Basis Function (RBF) kernel, was trained. Particularly in the field of epileptic seizure detection, SVM with RBF have been associated to very satisfactory results, often superior to the state-of-the-art, both in limited-channel and high-density configurations, e.g. [11, 2, 17].

The hyperparameter tuning of the regularization parameter (C) and kernel coefficient ($gamma$) was performed by grid search, with 5-fold cross validation (using the logarithmic grids $C = [10, 1, 0.1]$ and $gamma = [0.1, 0.01, 0.001]$, which provide a relatively large range).

2-fold testing: Testing was performed in two different ways: offline and online. Online testing simulates an online classification procedure, i.e. for each sample received by the classifier, one label is assigned. It also has an additional step in the classification pipeline: a temporal constraint of 6 seconds [2] for the classification of seizures and the re-classification (to seizure) of single background samples within seizure samples.

6.4. Results

Hyperparameters: The best hyperparameters were chosen as the ones that obtained the best overall score across the 5 cross validations, performed during training. Interestingly, within the same montage, the values of the regularization

[2] Literature reports that EEG abnormalities are required to persist for a minimum of 6-10 seconds in order to be considered a seizure. [14]

Table 4: Summary of the number of test samples after the splitting procedure described above. The first row indicates the dataset to which the subsets belong. With these values we can infer how balanced the test subsets are and how close they correspond to 20% of the seizure samples. Note: ABSZ and MYSZ from *0103* did not have enough seizure samples, hence why they were not included in the analysis.

	0103			**02**		
	bckg	**sz**	**target**	**bckg**	**sz**	**target**
FNSZ	4149	5355	20849	1830	2894	3206
GNSZ	5321	5301	8820	2952	5290	2953
SPSZ	476	248	424	–	–	–
CPSZ	5662	4237	5777	1367	1269	1245
ABSZ	–	–	3	1089	139	159
TNSZ	229	69	235	–	–	—
TCSZ	517	436	448	723	542	658
MYSZ	–	–	4	628	606	258

parameter were consistent across seizure types ($C = 1$ for *0103* and $C = 10$ for *02*). Similarly, the kernel coefficients were the same for both montages, assuming an intermediate value, meaning each sample does not have a very large nor very small range of influence in classification. Nonetheless, we can observe that the regularization parameter is larger for montage *02*. From this, we can infer that montage *0103* has overall less separability between classes, which implies a larger regularization to avoid overfitting to the training samples.

Test results: The results from the framework described above allow for three different frames of analysis: 1) The feasibility of the proposed electrode configuration in detecting each type of seizure, independently; 2) The added value of the correction implementation using temporal constraints; and 3) The impact of the reference electrode. Table 5 shows the classification results for the test subsets, using the best hyperparameters. The values correspond to the average of F1-scores across seizure and background classes.

Table 5: Classification results for the test subsets, using the best hyperparameters, defined above. The values correspond to the average of F1-scores, averaged over seizure and background classes (in %).

	0103		**02**	
	offline	**online**	**offline**	**online**
FNSZ	79.9	83.5	70.1	72.5
GNSZ	53.3	51.0	60.6	61.6
SPSZ	47.1	40.8	–	–
CPSZ	41.3	42.4	62.2	63.3
ABSZ	–	–	74.6	82.2
TNSZ	30.7	29.3	–	–
TCSZ	73.9	78.9	99.2	99.5
MYSZ	–	–	93.4	99.0

We can start by acknowledging that the online format of classification, which includes the correction algorithm, is consistently superior to its offline counterpart (except for GNSZ, SPSZ and TNSZ of montage *0103*). To validate this inference, a Wilcoxon signed-rank test for pairwise testing was adopted, under the null hypothesis that the median of the differences in performances (between offline and online) was positive against the alternative that it was negative. The test showed that the correction algorithm elicited a statistically significant improvement in the performance of the classification using the subsets from montage *02* ($w = 0.0$, $p = 0.02$), but not from montage *0103* ($w = 11.0$, $p = 0.58$).

Given this, it is also interesting to note that montage *02* has overall better results than montage *0103* (except for the detection of FNSZ), which again reflects the overlap between classes in *0103*. This contributes to the initial assumption that the reference used in the montage does have the potential to significantly impact the classification, even after re-referencing. However, contrary to the reference used in *0103* (Average Reference), the reference used in *02* (Linked-Ears Reference) is largely similar to the one in EmotAI's headband (Left Ear Reference). Therefore, the fact that this montage exhibits better results is encouraging in regards to the proposed future implementations.

Considering the evidence of the effect of the montage, the analysis regarding the individual seizure types will be focused on montage *02* alone. Table 6 shows a more comprehensive group of performance measures for montage *02* with online testing.

Although FNSZ was not the type of seizure with best performance, the reported results are satisfactory, with an almost perfect sensitivity to seizure events, albeit with a significant presence of false positives. Similarly, ABSZ shows a large sensitivity, comparable to the one reported in [11], for the detection of absence seizures, using the same electrode configuration (sensitivity: 93.7%). However, the test results show a significantly lower precision than that of [11] (precision: 86.7%).

Table 6: Classification results for montage *02*, with the online testing format (including the correction algorithm). Acc: Accuracy, Sn: Sensitivity, P: Precision.

	Acc %	**Sn %**	**P %**
FNSZ	77.8	99.4	73.6
GNSZ	64.0	41.5	69.3
CPSZ	63.5	57.9	63.2
ABSZ	90.5	98.6	54.4
TCSZ	99.5	98.9	100
MYSZ	99.0	98.2	99.8

Considering that GNSZ and CPSZ display considerably lower overall performances than that of the remaining types of seizures, can lead us to infer that the chosen configuration of electrodes cancels out the relevant electric patterns that would be crucial to distinguish between a seizure event and background. Although montage *02* did not have any SPSZ or TNSZ events, the results obtained with *0103* indicate the performances would likely be similar to GNSZ and CPSZ. Nevertheless, it is relevant to notice that CPSZ and SPSZ, like FNSZ, are very broad categories of seizures, in the sense that they can have several different focalities, which can result in contrasting detection performances for different seizure onset localizations and, therefore, overall lower performance.

As anticipated during the analysis of the overlap coefficients, the best overall performance was found for TCSZ, closely followed by MYSZ, with performances comparable (and in most cases, superior) to the state of the art reported for limited channel configurations, as evidenced in Table 7.

7. Achievements

With this work we showed that it is possible to automatically detect Tonic-Clonic Seizures and Myoclonic Seizures using the limited channel configuration of *Fp1-Fp2*. The algorithms designed for these two seizure types achieved sensitivities of 98.9% and 98.2%, as well as precisions of 100% and 99.8%, respectively, in the task of distinguishing between non-ictal and ictal samples. These results are incredibly satisfactory, representing performances comparable (and in most cases superior) to the state-of-the-art of similar works.

Furthermore, it also suggested the possibility of extending this detection to Focal Non-Specific Seizures and Absence Seizures, with further analysis regarding these two seizure types, as they achieved moderately adequate performances. They reported very high sensitivities of 99.4% and 98.6%, but disappointingly low precisions of 73.6% and 54.4%. These results clearly indicate the need to improve the representation of the background class, as it was typically mistaken by seizure samples. Additionally, the obtained results suggest that this particular channel configuration might not be adequate to detect Generalized Seizures, Complex Partial Seizures, Simple Partial Seizures and Tonic Seizures, considering their overall lower performance results in all testing configurations.

By performing separate analysis for each montage, we were able to verify the impact of the reference electrode in the overall classification task, showing that the montage with Linked-Ears Reference (LE) has consistently better performances than the one with Average Reference (AR). Nevertheless, these results are promising, since the proposed future implementations of the detection algorithm are intended for EmotAI's headband: a limited-channel EEG acquisition wearable, with a reference electrode very similar to LE (i.e. Left-Ear Reference).

Regarding the autonomous system for data acquisition, *EpiBOX* operates as a standalone unit that acquires, displays and stores up to 12 different biosignal channels, simultaneously. It operates within a private wireless network, in which an MQTT broker was successfully established, guaranteeing the communication between the UI and the autonomous recording unit (Raspberry Pi). A preliminary technical characterization of *EpiBOX* was performed, indicating satisfactory properties of the system, including a large efficiency in the acquisition (with only 0.3% of non-covered acquisition time), moderate memory usage and energy consumption, adequate WiFi speed to provide near-real time transfer between the acquisition device and the UI, estimated as 0.165 ms, as well as a suitable Bluetooth range to operate within an inpatient monitoring visit or home environment.

Furthermore, *EpiBOX* addresses all the issues identified in the currently available biosignal acquisition tool within Instituto de Telecomunicações (IT), as it guarantees the same acquisition flexibility (imposing no restrictions in terms of which signals to acquire, nor relating to acquisition configurations); while, at the same time, providing a simple interface, which enables the acquisition by non-technical personnel, contained within a $(82 \times 108)mm$ case.

Despite some efforts that still remain to achieve the ultimate goal of this work, this dissertation supports the potential applicability and encourages further research in the use of EmotAI's headband in the automatic detection of TCSZ, MYSZ (and potentially FNSZ and ABSZ). Furthermore, it simultaneously provides all the necessary ground work to implement the prospected autonomous system for continuous data acquisition, integrated with the obtained automatic seizure detection algorithms.

Table 7: Table of comparison between the results of this work and previous homologous works. (*): patient-specific approach, N.S.: Not Specified. Acc: Accuracy, Sn: Sensitivity, P: Precision, Sp: Specificity.

	Seizures	Channels	Acc (%)	Sn (%)	P (%)	Sp (%)
This work	TCSZ MYSZ	Fp1-Fp2	99.5 99.0	98.9 98.2	100 99.8	99.2 98.3
[5] (*)	N.S.	3 channels	–	80.87	40.47	–
[10] (*)	N.S.	1 channel 2 channels	93.5 95.2	–	–	–
[11]	ABSZ	F7-FP1 F7-F3 Fp1-Fp2	–	99.1 99.1 93.7	94.8 90.2 86.7	–
[8]	GNSZ	Fp2-F8	92.68	–	–	–
[16]	N.S.	F8-T4, F7-T3	–	93.80	–	93.37
[12]	N.S.	P4-O2, C3-Cz	–	31.15	–	40.82

8. Practical Guidelines for Future Work

This dissertation belongs to a larger collaborative work, within IT, which intends to research and develop technological solutions to mitigate several drawbacks in the field of epilepsy. This work in particular acts as the necessary stepping stone to achieve one of the goals of providing a fully automated seizure detection system with continuous monitoring and biosignal acquisition.

With that in mind, future work should start with three angles of action: 1) Carry out a usability testing phase, which should enable the detection of limitations and potential improvements of the proposed acquisition system, with the purpose of optimizing the user experience during handling of *EpiBOX*; 2) build upon the presented mobile app to create a patient version, integrated with a seizure diary, thus providing environmental context for the recorded seizures; and 3) Initiate the assembly of an EEG dataset with the use of EmotAI's headband.

The third task envisions the study of the applicability of the automatic detection algorithms that were developed within this dissertation to the data acquired with the wearable device. Although this work reports encouraging results using the channel *Fp1-Fp2* for the detection of TCSZ, MYSZ (and potentially FNSZ and ABSZ), performing a similar study with data acquired with the actual device is crucial to take accurate conclusions on the subject.

Furthermore, an interesting analysis (that was unfortunately not possible to perform in this work) is the study of the impact of epoch length in the automatic detection. The author suggests the use of the present research as ground work to select a smaller set of features, in order to decrease the time necessary for feature extraction and consequently enabling this more comprehensive analysis. Other pertinent considerations include the investigation of alternative limited-channel configurations to surpass the limitations identified in this work, particularly considering the detection of GNSZ, CPSZ, SPSZ and TNSZ.

Additionally, the advantages of using multimodal approaches in seizure detection and prediction have been acknowledged in several studies [1]. Therefore, the author encourages the use of *EpiBOX* for simultaneous acquisition of EEG and other modalities, to further investigate the effect of such approaches in the scope of epileptic seizures.

Finally, it is impossible to not recognize the invaluable advantages of seizure prediction, i.e. anticipating when a seizure will occur, based on the dynamics of pre-ictal periods [1, 3]. Hence, it is undeniable that this work will eventually culminate in a fully automated seizure prediction system, also with several efforts within the research team of IT being directed towards this reality. Nevertheless, all the work done in this dissertation serves either as a complementary tool to this objective (namely, *EpiBOX*) or as a background research to build useful knowledge upon.

9. Acknowledgments

This document was written and made publicly available as an institutional academic requirement and as a part of the evaluation of the MSc thesis in Biomedical Engineering of the author at Instituto Superior Técnico. The work presented in this thesis was performed at Institute of Telecommunications, Instituto Superior Técnico (Lisbon, Portugal), during the period February 2020 - January 2021, under the supervision of Prof. Ana Luísa Nobre Fred and Prof. Hugo Plácido da Silva and co-supervised by Dra. Carla Bentes, from Hospital de Santa Maria.

References

[1] M. Abreu, A. Fred, H. Plácido da Silva, and C. Wang. From Seizure Detection to Prediction: A Review of Wearables and Related Devices Applicable to Epilepsy via Peripheral Measurements. Technical Report IT-FMCI-20190905, Institute of Telecommunications, 03 2020.

[2] U. R. Acharya, R. Yanti, G. Swapna, V. S. Sree, R. J. Martis, and J. S. Suri. Automated Diagnosis of Epileptic Electroencephalogram Using Independent Component Analysis and Discrete Wavelet Transform for Different Electroencephalogram Durations. *Proc. of the Institution of Mechanical Engineers. Part H, Journal of Engineering in Medicine*, 227(3):234–244, 2013.

[3] H. Agboola, C. Solebo, D. Aribike, A. Lesi, and A. Susu. Seizure Prediction with Adaptive Feature Representation Learning. *Journal of Neurology and Neuroscience*, 10:294, jan 2019.

[4] D. Batista, H. P. Silva, A. Fred, C. Moreira, M. Reis, and H. A. Ferreira. Benchmarking of the BITalino Biomedical Toolkit Against an Established Gold Standard. *Healthcare Technology Letters*, 6:32–36, 2019.

[5] J. Birjandtalab, M. Baran Pouyan, D. Cogan, M. Nourani, and J. Harvey. Automated Seizure Detection Using Limited-Channel EEG and Non-Linear Dimension Reduction. *Computers in Biology and Medicine*, 82:49–58, 2017.

[6] S. Ferrell, , V. Mathew, M. Refford, V. Tchiong, T. Ahsan, I. Obeid, and J. Picone. *The Temple University Hospital EEG Corpus: Electrode Location and Channel Labels*. The Neural Engineering Data Consortium, July 2019.

[7] K. Kutt, W. Binek, P. Misiak, G. Nalepa, and S. Bobek. Towards the Development of Sensor Platform for Processing Physiological Data from Wearable Sensors. In *Proc. of the 17th Int'l Conf. on Artificial Intelligence and Soft Computing 2018*, pages 168–178, 06 2018.

[8] S.-K. Lin, Istiqomah, L.-C. Wang, C.-Y. Lin, and H. Chiueh. An Ultra-Low Power Smart Headband for Real-Time Epileptic Seizure Detection. *IEEE journal of Translational Engineering in Health and Medicine*, 6:2700410, aug 2018.

[9] S. López, A. Gross, S. Yang, M. Golmohammadi, I. Obeid, and J. Picone. An Analysis of Two Common Reference Points for EEGs. *IEEE Signal Processing in Medicine and Biology Symposium (SPMB)*, 2016:10.1109/SPMB.2016.7846854, dec 2016.

[10] L. A. Moctezuma and M. Molinas. EEG Channel-Selection Method for Epileptic-Seizure Classification Based on Multi-Objective Optimization. *Frontiers in Neuroscience*, 14:593, 2020.

[11] E. B. Petersen, J. Duun-Henriksen, A. Mazzaretto, T. W. Kjær, C. E. Thomsen, and H. B. D. Sorensen. Generic Single-Channel Detection of Absence Seizures. In *Proc. of the 2011 Annual Int'l Conf. of the IEEE Engineering in Medicine and Biology Society*, pages 4820–4823, 2011.

[12] V. Shah, M. Golmohammadi, S. Ziyabari, E. Von Weltin, I. Obeid, and J. Picone. Optimizing Channel Selection for Seizure Detection. In *Proc. of the 2017 IEEE Signal Processing in Medicine and Biology Symposium (SPMB)*, pages 1–5, 2017.

[13] V. Shah, E. von Weltin, S. Lopez, J. McHugh, L. Veloso, M. Golmohammadi, I. Obeid, and J. Picone. The Temple University Hospital Seizure Detection Corpus. *Frontiers in Neuroinformatics*, 12:83, 01 2018.

[14] A. Shoeb and J. Guttag. Application of Machine Learning To Epileptic Seizure Detection. In *Proc. of the 27th Int'l Conf. on Machine Learning 2010*, pages 975–982, aug 2010.

[15] A. H. Shoeb. *Application of Machine Learning to Epileptic Seizure Onset Detection and Treatment*. PhD thesis, Massachusetts Institute of Technology, sep 2009.

[16] D. Sopic, A. Aminifar, and D. Atienza. e-Glass: A Wearable System for Real-Time Detection of Epileptic Seizures. In *Proc. of the 2018 IEEE Int'l Symp. on Circuits and Systems (ISCAS)*, pages 1–5, May 2018.

[17] A. Subasi and M. Ismail Gursoy. EEG Signal Classification Using PCA, ICA, LDA and Support Vector Machines. *Expert Systems with Applications*, 37(12):8659 – 8666, 2010.

[18] A. Widmann, E. Schröger, and B. Maess. Digital Filter Design for Electrophysiological Data – A Practical Approach. *Journal of Neuroscience Methods*, 250:34 – 46, 2015.